

Inorganic Nanocomposite Solar Cells by Atomic Layer Deposition (ALD)

Investigators

Stacey Bent, Professor, Department of Chemical Engineering; James Harris, Professor, Department of Electrical Engineering; Michael McGehee, Associate Professor, Department of Materials Science and Engineering; Bruce Clemens, Professor, Department of Materials Science and Engineering; Jeffrey King, David Jackrel, Post-Doctoral Researchers; Evan Pickett, Michael Rowell, Vardan Chawla, Randy Groves, Graduate Researchers

Abstract

This project is a fundamental study into the development of low-cost, thin film solar cells. It explores the fabrication of semiconductor nanocomposites for photovoltaics using nanostructured inorganic materials and atomic layer deposition (ALD). In thin film technologies, there exists a common problem with conversion efficiency due to poor materials quality: the photogenerated electrons and holes cannot travel very far before recombination (short free-carrier diffusion lengths) and are hence lost for power conversion. If the solar cell can be made using nanoscale heterojunctions, then every photogenerated carrier will have less distance to travel, and the problem of recombination can be greatly reduced. The proposed designs allow collection of all photogenerated carriers even in poor quality materials, thus making low cost deposition routes acceptable. We have performed modeling studies on single and multijunction device geometries which show that the negative effects of short minority-carrier lifetimes, namely high dark current, will be exacerbated by the large increase in junction area that occurs with nanostructuring. As a result, it appears that a good candidate for nanostructuring would be a material where low mobility—not short lifetimes—is the reason for low diffusion length. Another solution is to relax the size scale for the nanostructuring, from 100 nm to 100's of nanometers or even a few microns. This will allow a compromise to be reached between collecting the maximum number of carriers and minimizing the interface area. Current plans call for absorber material based on $\text{Cu}_2\text{ZnSnS}_4$ to be incorporated into nanostructured devices both by sputtering and chemical bath deposition (CBD), either through deposition on a nanostructured substrate or through nanostructuring of planar films. The opposite polarity material will be deposited by both ALD and by CBD. Nanostructured templates of both hole and pillar arrays have been successfully formed on silicon by using nanosphere lithography and reactive ion etching. Progress in development of low cost methods of deposition of the semiconductor thin film has been made, based on techniques that utilize chemical bath deposition, ion exchange, and sulfidization. Future work will also include films grown by sputter deposition combined with sulfidization. Several tools are being developed to make or study the nanocomposite solar cells, including an ALD reactor, sputter deposition system, sulfidization apparatus, and a scanning probe microscope.

Introduction

This project is a fundamental study into the development of low-cost, thin film solar cells. It explores the fabrication of semiconductor nanocomposites for photovoltaics using nanostructured inorganic materials and atomic layer deposition (ALD). The focus is on cells built by high-throughput techniques where nanoporous structures, ultrathin layers, and multiple junctions are used to achieve good energy conversion efficiencies at low cost. This report will describe the progress we have made on several fronts, including fabrication of nanostructured templates, deposition of inorganic semiconducting materials, and development of several tools needed to make or study the nanocomposite solar cells, including an ALD reactor, sputter deposition system, sulfidization apparatus, and a scanning probe microscope.

Background

There is a strong need for the development of photovoltaic cells with low cost, high efficiency, and good stability. In thin film technologies, there exists a common problem with conversion efficiency due to poor materials quality: the photogenerated electrons and holes cannot travel very far before recombination (short free-carrier diffusion lengths) and are hence lost for power conversion. If the solar cell can be made using nanoscale heterojunctions, then every photogenerated carrier will have less distance to travel, and the problem of recombination can be greatly reduced. ALD is particularly well suited for this application since it can allow for highly uniform deposition on complex non-planar nanostructures with controllable thickness. For somewhat larger dimensions (100 nm to a few microns), other inexpensive deposition methods may also be employed. With short diffusion lengths for the photogenerated carriers, the materials constraints can be relaxed, and low cost deposition routes become acceptable.

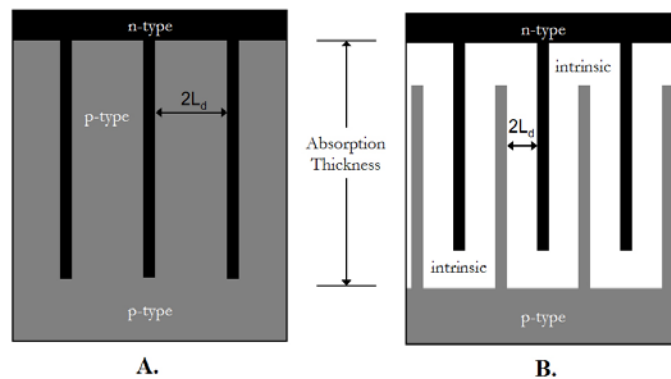


Figure 1: Cross-sections of nanointerpenetrated p/n junction solar cell geometries, each requiring different nanofabrication; L_d is the minority carrier diffusion length. A) Heterojunction geometry; nanoholes are etched into a planar p-type absorber, then the n-type window is conformally deposited by ALD or CBD. B) PIN geometry; p-type material is first nanostructured into pillars, then the intrinsic absorber and n-type window are conformally coated.

Figure 1 illustrates two proposed geometries for single junction solar cells that provide long absorption lengths and short photogenerated carrier paths. By

nanostructuring at the correct length scale, the photogenerated carrier path-lengths can be kept below the minority carrier diffusion length, greatly reducing bulk recombination.

Results

There are three major issues which must be addressed in the proposed solar cells. First is the development of the nanostructured substrates (or absorbers) with variable pore size and morphology. Second is the issue of deposition of the other material forming the p/n junction and the subsequent growth of additional layers, such as compound semiconductors, into the nanostructured substrate. The third challenge is the electrical connection and current collection from all of the nanostructured p/n junctions.

Nanostructuring - Fabrication

The nanostructured substrates (or absorbers) could potentially be fabricated by three techniques: nanosphere lithography, laser interference (or holographic) lithography, or anodization of a metal such as aluminum.[1-3] The primary reason for nanostructuring is to create a device that is optically thick to efficiently absorb the incident sunlight, and to simultaneously have every photogenerated electron-hole pair be very close to the p/n junction with respect to the minority carrier diffusion length, to minimize recombination losses. The minority carrier diffusion length in high quality silicon can be as long as 1 mm, and only a few hundred microns of material are needed to absorb over 95% of the incident light. As a result, high quality silicon devices have achieved efficiencies near their theoretical limit. With poor quality (i.e. cheaply deposited) inorganic semiconductors, the diffusion length can be on the order of only 100 nm, while the absorption length is a micron at best. This leads to poor efficiencies in planar solar cells made from these materials, since only a small fraction of the sunlight is absorbed within a minority carrier diffusion length of the p/n junction, and many of the photogenerated minority carriers recombine before reaching the junction. Nanostructuring addresses this problem, provided the pore radius of the nanostructures is on the order of the minority carrier diffusion length. Nanosphere lithography is well-established for the 100 – 500 nm length scales, and interference lithography for length scales above about 200 nm. Some preliminary studies using 100 nm and 200 nm carboxylated polystyrene nanospheres to pattern crystalline and amorphous silicon substrates have been done.

The nano-interpenetrated p-type/intrinsic/n-type (PIN) structure (Fig. 1B) is fabricated by first nanostructuring the substrate (p-type in Fig. 1) into spaced *nanopillars* (rather than *nanoholes*) and then the absorbing intrinsic layer and n-type layer are conformally deposited into the nanostructure. The intrinsic layer is kept thin enough to not planarize the structure. The n-type film above then planarizes the structures, allowing the top electrical contact to be more easily deposited. The nano-interpenetrated p-n junction (Fig. 1A) is fabricated by nanostructuring an array of spaced holes into the absorber layer. The n-type layer is then deposited conformally into the holes. In either structure, thin interface layers could be grown in between the layers to reduce recombination at the large surface area junction. [2, 4]

We have fabricated both nanopillars and nanoholes in silicon using nanosphere lithography and reactive ion etching (RIE). Close-packed arrays of both holes and pillars

were fabricated using 200 – 500 nm diameter surface-modified (carboxylated) polystyrene spheres. The spheres were spin coated, and RIE was performed with an Applied Materials Precision 5000 plasma etcher using standard silicon etching conditions. Ordered arrays of pillars were fabricated using polystyrene spheres as the etch mask in RIE. Arrays of holes were fabricated by first reducing the sphere diameter using an oxygen plasma etch, then depositing chromium and performing liftoff in toluene to remove the spheres. The film with chromium mask was then etched in RIE, and the holes in the metal (where the spheres had been) became etched into the silicon. Figure 2 shows SEM images of spheres spun onto silicon before (Fig. 2A) and after (Fig. 2C) diameter reduction, as well as after RIE to create both pillar (Fig. 2B) and hole arrays (Fig. 2D). Studies are underway to optimize the dimensions of both the nanopillar and nanohole arrays, with respect to both diameter to period ratio and aspect ratio.

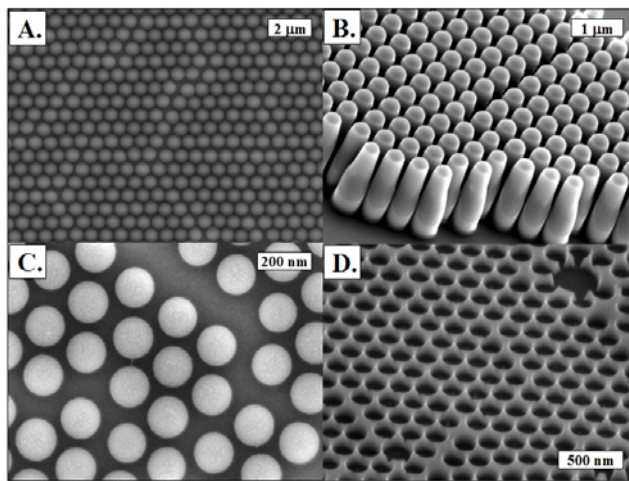


Figure 2: SEM images of nanospheres (NS) and RIE etched nanostructures in silicon. A) 500 nm diameter carboxylated polystyrene NS spin-coated on silicon substrate. B) Nanopillars created by RIE from NS mask in Fig 2A. C) 200 nm NS spun onto silicon and etched in oxygen plasma to reduce their diameters to roughly 150 nm. D) Nanoholes in silicon created from NS array in Fig. 2C using chromium etch mask during RIE..

Nanostructured PV – Design Calculations

The second major challenge is the deposition of the other material forming the p/n junction into the nanostructured substrate, and the larger concern of what solar cell materials are appropriate to nanostructure in general. A major thrust of the project work has been focused on theoretical modeling in order to determine materials design parameters. We have performed modeling studies on single and multijunction device geometries, buffer layers, pore dimensions, and materials electrical and optical properties, such as bandgap, free-carrier mobility, free-carrier lifetime, doping density, and dielectric constant. Thus far the electrical properties have been modeled in a 1-D geometry (using the modeling program AMPS), or evaluated using models from the literature, but future work may use a 2-D and 3-D modeling program (DESSIS) in order to more fully investigate the effects of different nanostructure geometries and the effects of materials parameters on nanostructured devices.[4,5,6] Buffer layers that could be used to reduce

the recombination at the p/n junction were 1-D modeled to evaluate different buffer layer/device materials combinations.

In terms of selecting a materials system for use in the nanostructured design, the device performance of a candidate material should be limited by the minority carrier diffusion length in planar structures, since this is the problem that nanostructuring addresses. There are many inorganic solar cell materials that have short diffusion lengths when deposited cheaply; these methods often lead to small grain polycrystalline material, or large impurity concentrations (point defects). The diffusion length, L_D , can be determined from the carrier lifetime, τ , and the diffusion coefficient or the mobility, D and μ , respectively:

$$L_D = \sqrt{D\tau} \sim \sqrt{\mu\tau} \quad (1)$$

A short effective diffusion length can be caused by either a low mobility or a low lifetime, and these two properties are not necessarily related to each other. Quite often, these short diffusion lengths are the result of recombination through traps which leads to short minority-carrier lifetimes. Unfortunately, the negative effects of short minority-carrier lifetimes, namely high dark current, will be greatly exacerbated by the large increase in junction area that occurs with nanostructuring. As a result, it appears that a good candidate for nanostructuring would be a material where low mobility—not short lifetimes—is the reason for low diffusion length, such as hydrogenated amorphous silicon (a-Si:H). Kayes, et al. pointed out in 2005 that, somewhat counter-intuitively, a material that has a high free-carrier mobility, such as crystalline silicon or GaAs, would have excessive leakage current in a nanostructured interpenetrated p/n junction geometry; this would cause the open-circuit voltage, and thus the efficiency, to drop almost to zero.[5] Another solution is to relax the size scale for the nanostructuring, from 100 nm to 100's of nanometers or even a few microns. This will allow a compromise to be reached between collecting the maximum number of carriers and minimizing the junction (interface) area. We are currently exploring this approach.

Deposition of Semiconducting Materials

For our PV studies, we chose to investigate the I₂-II-IV-VI₄ class of materials. This class can be conceptualized by starting from the I-III-VI₂ class (i.e. Cu₂InGaSe₄) and splitting the group III element into one group II and one group IV element to maintain an average of four valence electrons per constituent atom. There is one possible candidate material from this class, Cu₂ZnSnS₄ (CZTS), which has an attractive bandgap of 1.4-1.5 eV. CZTS is a material that is comprised of abundant, non-toxic elements that has potential application in conventional thin film as well as nanostructured photovoltaic systems. The photovoltaic materials will be deposited by both ALD and by chemical bath deposition.[7] An ALD reactor is being built to deposit the semiconductor materials (as described later in report). In addition, we are exploring the possibility of depositing the materials by sputter deposition.

We are preparing to deposit Cu, Sn and ZnS layers by sputter deposition onto Mo-coated glass substrates followed by sulfidization of the layers by annealing at roughly

500-600°C in a hydrogen sulfide environment. We also are investigating, in parallel, alternative methods of film deposition that lend themselves to low-cost high-throughput processing. Specifically, we have made progress in developing a wet chemical approach based on chemical bath deposition (CBD) of Cu₂S, SnS, and ZnS layers. A three layer stack design, incorporating discrete Cu₂S, ZnS, and SnS layers is being developed. In addition, an approach based on ion exchange has shown promising results.[8] Using this method, a single layer of ZnS is deposited by CBD, and subsequent exposure to concentrated solutions containing Sn²⁺ and Cu²⁺ ions, both of which have higher standard reduction potentials than Zn²⁺, yields incorporation of these ions into the semiconducting film via ion exchange. After deposition of the precursor layers, sulfidization anneals at roughly 500-600°C have been performed in a hydrogen sulfide environment to convert the layers into polycrystalline Cu_xZn_xSn_zS films. In addition to the CZTS based materials, we have also been investigating the CBD of CdS, which is the standard window layer for quaternary PV modules such as CIGS.

CBD is a solution-based deposition technique used for economical growth of thin films on a variety of substrates. The method is applicable for many different materials, including oxides and sulfides.[7] It is a well-established technique used commercially for growth of CdS films in both CIGS and CdTe photovoltaic modules. This technique involves the growth of films from a solution comprised of metal salts, sulfur-containing chemicals (e.g. thiourea), and various complexing agents. It is applicable to a wide range of materials, including Cu₂S, ZnS, and SnS. For example, in a relevant example, Nair et al. produced CuSnS thin films by heating SnS-CuS layers deposited by chemical bath.[9] We have successfully grown both CdS and ZnS by CBD, and are making progress toward growth of SnS and Cu_xS as well.

For CBD growth of CdS, a substrate was immersed in a hot (60 – 100 °C), well-stirred aqueous solution containing cadmium salt, a sulfur source (e.g. thiourea), an ammonia salt, and ammonia hydroxide. For our experiments, the deposition bath was maintained at 85 °C and contained cadmium sulfate, ammonium sulfate, thiourea, ammonium hydroxide, and deionized water. Test structures of monocrystalline p-type silicon were nanostructured via nanosphere lithography, and a ~ 100 nm thick n-type CdS film was then deposited on the structure, as shown in Figure 3 below. Figure 4 shows XPS analysis of the film after a 20 second argon sputter which indicates a composition of 51% Cd, 29 % S, and 20 % O. The film contains a large amount of oxygen, likely in the form of cadmium hydroxide. ZnS was grown via two different bath compositions. The first consisted of ZnSO₄, pH 10 buffer solution, triethanolamine, thiourea, and deionized water and yielded 100 – 200 nm films for overnight growth at room temperature.[10] The second consisted of ZnSO₄, ammonium hydroxide, thiourea, and DI water, and yielded ~500 nm films in 45 minutes from baths maintained at 80°C, as shown in Figure 5.[11] Figure 6 shows XPS analysis of the film after a 20 second argon sputter indicates a composition of 42.3 % Zn, 27.2 % S, and 30.5 % O. As with CdS, the film contains a large amount of oxygen. In addition to ZnS and CdS, experiments are underway to grow both SnS and Cu_xS by CBD.

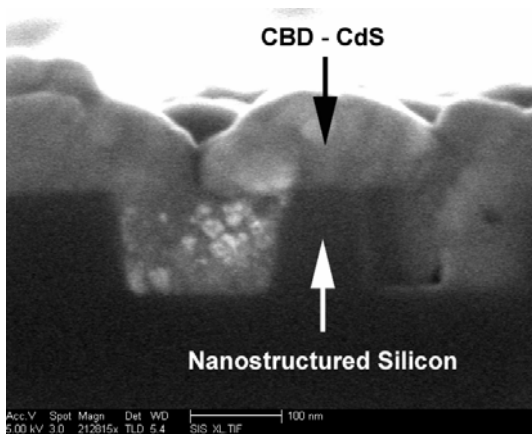


Figure 3. Cross sectional SEM image of CdS/Si nanostructured p-n junction at higher magnification.

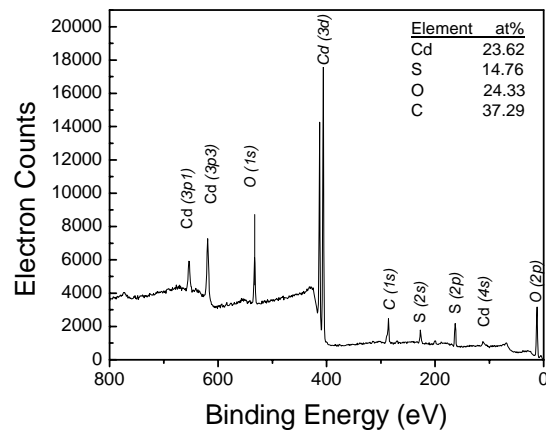


Figure 4. XPS analysis of CdS film deposited by CBD.

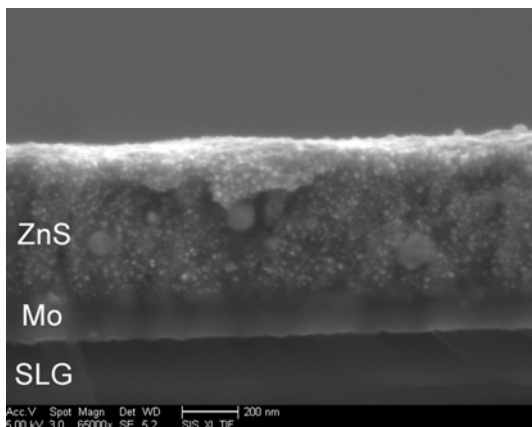


Figure 5. Cross sectional SEM image of ZnS film deposited via CBD.

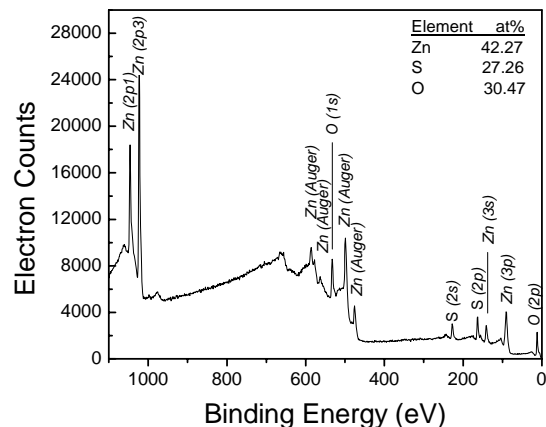


Figure 6. XPS analysis of ZnS film deposited via CBD.

Both Sn and Cu have been incorporated into CBD ZnS films via ion exchange. For Sn, the ZnS film was soaked in a saturated aqueous solution of SnCl_2 for 1 minute. The film was next soaked in a 0.1 M CuCl_2 aqueous solution. The resulting film was analyzed by XPS. Ar sputtering was used to obtain an elemental depth profile. At the surface, the concentration of Zn:Cu ratio of 1.4, while the Zn:Sn ratio was 0.12, indicating considerably more Sn incorporation than Cu. Figure 7 shows the resulting XPS spectra from this sample. After 155 sec of sputtering the Zn:Cu ratio was still 1.4, while the Zn:Sn ratio increased to 0.25. Thus, the copper incorporation is more uniform than the Sn, which shows higher concentration near the surface.

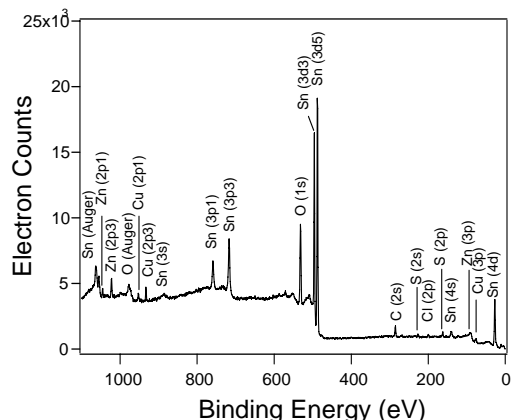


Figure 7: XPS Spectra of $\text{Cu}_x\text{Zn}_y\text{Sn}_z(\text{O,S})$ film formed by CBD and ion exchange

Post-deposition sulfidization heat treatments were performed on CBD deposited films. The sulfidization chamber is described in more detail in the next section of the report. Exposure of as-deposited $\text{Zn}(\text{O,S})$ films to a H_2S environment for 2 hours at 500°C facilitated removal of oxygen and conversion of the films to stoichiometric ZnS . An SEM image of the film surface is shown in Figure 8 and XPS analysis is shown in Figure 9.

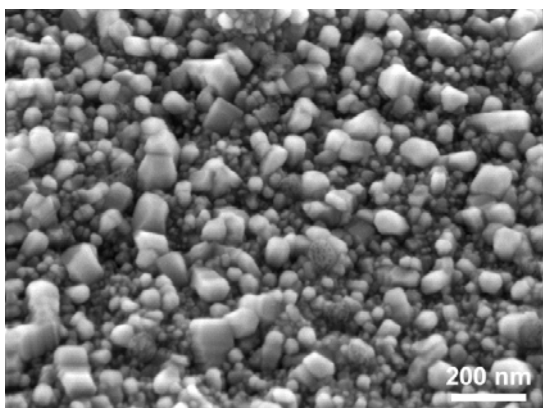


Figure 8. SEM image of ZnS film surface after 2 hour H_2S heat treatment.

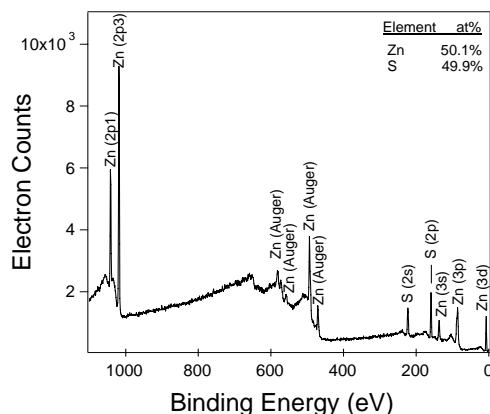


Figure 9. XPS analysis of ZnS film after 2 hour H_2S heat treatment.

Apparatus for depositing and testing nanocomposite PV materials ALD reactor progress

A viscous flow, cold wall ALD reactor is being designed and built. The system will have capacity for as many as six individual computer-controlled precursor lines, giving a large degree of flexibility in materials choice. For example, the ability to grow different materials without a vacuum break will allow study of the effects of buffer layers and interfacial layers designed to minimize interfacial recombination. The reactor is being designed to be capable of deposition temperatures in excess of 500°C , and will be capable of delivery of liquid, solid, and gaseous precursors for growth of both compound semiconductors (including sulfides) and metal oxides. In addition, the reactor will incorporate a quartz crystal microbalance for in-situ growth analysis.

Sputter deposition system

In order to prepare samples of new materials such as CZTS, we are constructing a multi-target sputter deposition facility for growth of photovoltaic materials. This facility will include in-situ substrate heating, a three target sputter source, a separate chamber with two additional sources for depositing Mo and Cr underlayer films, and a third chamber for post-deposition treatment. This system will be used to deposit films with a nominal composition around $\text{Cu}_2\text{ZnSnS}_4$ – a promising new photovoltaic material, as described above.[12] In order to minimize the defects associated with out-diffusion of metals during post-deposition sulfidization treatment we will use sulfide targets to maximize the sulfur content of as-deposited films. We will also investigate reactive sputtering with either H_2S or an evaporative sulfur source.

Sulfidization

A sulfidization reactor has been constructed for heat treatment of both CBD and sputtered precursor films. The chamber is a cold wall design, constructed of stainless steel. An internal DC stage heater regulated by a PID temperature controller is incorporated, and is capable of temperatures in excess of 500°C . The reactor is evacuated using a rotary vane pump, which allows a base pressure of 10 mTorr. A mass flow controller is used to control the flow of inert gas (nitrogen) in the reactor. During sulfidization heat treatments, the vacuum line is closed, and hydrogen sulfide gas is introduced into the reactor, bringing the pressure up to ~ 400 mTorr in a batch style, or static condition. Periodically, the reactor can be evacuated, and the H_2S refreshed. Preliminary results have shown this method to be quite effective for sulfidization.

Scanning Probe Microscopy

We are developing techniques for performing various scanned probe electrical measurements on inorganic materials as an addition to our characterization techniques. Scanning probe microscopy (SPM) has become an essential tool in the last 10 years in the understanding of thin film solar cells, in particular the CdS/CdTe/Cu and CIGS ($\text{Cu}(\text{In}_x\text{Ga}_{x-1})(\text{S},\text{Se})$) systems. SPM allows the direct mapping—both topographical and cross sectional—of properties such as work function, location of built in potentials and depletion zones, and photovoltage. This technique will be particularly crucial for nanostructured solar cells in that the three-dimensional, multi-interface nature of the device makes traditional methods of characterizing the electrical junction properties, such as capacitance-voltage data or modeling software, difficult or impossible to use. For example, for the device in Figure 1B, electrostatic force microscopy (EFM), which can measure the local work function and any variations in it due to electric fields from space charge, is the only way to observe the shape of the depletion region. This will be critical for optimizing the device structure, doping levels, and understanding the effect of any interface modifiers.

We will perform SPM studies on CIGS devices made in other labs in addition to our own devices. It has become apparent in the last several years that these thin film devices work “surprisingly” well because they are inherently nanostructured. As this project is focused on intelligently nanostructuring materials for increased efficiency, it is essential that we understand the known systems where nanostructuring is apparently beneficial,

and to understand why. To date, these nanoscale effects are not completely understood. Many theories to explain the surprising efficiency of CIGS cells have been put forth. They generally fall into two categories. The most recent theory describes a nanoscale (~10 nm) phase separation within the absorber that forms an interpenetrated bulk heterojunction.[13] This interpenetrated nanoscale junction spatially separates the carriers enough to reduce recombination. So far these nanodomains have only been observed by TEM and their electrical significance has not been verified. We are developing high resolution EFM modes and probe tips that will be capable of detecting these domains. A second group of theories explains the benign, or even favorable, presence of grain boundaries.[14] CIGS cells are polycrystalline and have grain boundaries every ~500 nm. Theories include a compositional change at the grain boundary causing a heterojunction that separates carriers or the presence of ions that also separate carriers; both scenarios result in reduced recombination in the absorber and enhanced carrier collection. What we learn from these studies will shape our design objectives in creating the ideal nanostructure.

Electrical Connection and Current Collection

The third challenge is the electrical connection and current collection from all of the nanostructured p/n junctions. The electrical connection will be made much simpler if the device structures can be planarized, either during or after growth. However, if the surface roughness is too great and standard metal evaporation is not sufficient to create a good electrical contact then alternative contact deposition techniques, such as screen-printing, will be investigated.

One of the biggest fundamental electrical challenges facing interpenetrated p/n junction nanostructured solar cells is the recombination at the p/n junction interface. Recombination scales linearly with the junction area, and in these cells the junction area can be orders of magnitude larger than a planar design with the same solar cross-section. There has been some work done depositing thin buffer layers (~10 nm) in between the p- and n-type materials in nanostructured cells to suppress interfacial recombination.[15,16] We performed 1-D modeling to evaluate the effects of different buffer layer/device materials combinations. It has been suggested that a buffer layer with appropriate conduction and valence band energies could reduce interfacial recombination by reducing free-carrier concentrations at the interface between the n- and p-type materials. This will increase the open-circuit voltage, but our modeling shows it comes at the cost of the device current; the lower carrier concentrations near the junction interface also reduce the electric field strength which is needed to collect the photogenerated carriers. We have therefore determined that much of the benefit of buffer layers observed in nanostructured interpenetrated p/n junction solar cells is likely the result of improved interface chemistry (passivation) at the junction, rather than an altering of electron and hole concentrations through band-level engineering.

Progress

We have made progress in development of potential nanostructured architectures and materials systems where these designs would offer significant efficiency enhancement in modules deposited using low-cost methods. It is anticipated that these architectures will

yield decreased cost per watt in PV modules, allowing for a shift in global energy generation toward clean, renewable carbon-free technologies. The current world record power conversion efficiency for single-junction hydrogenated amorphous silicon solar cells is just below 10%. [17] Our device modeling has shown that if nanostructuring enabled the cells to achieve 100% quantum efficiency, then the current could be increased from 16 mA/cm² up to 21.5 mA/cm², significantly increasing the open-circuit voltage as well, yielding a power conversion efficiency as high as 15%. We have also identified Cu₂ZnSnS₄ as a good test case for nanostructuring. Current state of the art planar cells allow efficiencies of ~5%, but it is anticipated that CIGS-like efficiencies close to 20% should be possible. Nanostructuring should allow attainment of this goal with lower demand on materials quality. These devices would be single-junction cells, manufactured largely with techniques amenable to high throughput processing. We are therefore moving towards the design and fabrication of a nanostructured solar cell that could be made using low-cost production techniques at efficiencies matching current thin-film devices, success of which would allow reduced dependence on fossil fuel energy production worldwide.

Future Plans

Nanostructured interpenetrated p/n junction solar cells will continue to be investigated. The nanostructured substrates (or absorbers) could potentially be fabricated by three techniques: nanosphere lithography, laser interference (or holographic) lithography, or anodization of a metal such as aluminum. From the results of our modeling, we have determined that interpenetrated junctions with dimensions on the order of 100's of nanometers to microns have the potential for improving the performance of devices with low materials quality. Current plans call for absorber material based on Cu₂ZnSnS₄, a good candidate material, to be incorporated into the nanostructured device both by sputtering and CBD, either through deposition on a nanostructured substrate or through nanostructuring of planar films. The opposite polarity material will be deposited by both ALD and by chemical bath deposition. We will complete the fabrication of both the ALD reactor and the sputter deposition system and use them to deposit the semiconducting materials on both planar and nanostructured substrates.

The materials properties and electrical device properties of each round of test structures will be characterized and modeled, and improvements in the materials and geometry will be incorporated into subsequent test structures. Future modeling studies will investigate nanostructure geometries and materials properties using the 2-D software DESSIS. Particularly, the effect of minority-carrier mobilities and lifetimes on the performance of solar cells with different nanostructures and interface properties will be investigated. Materials characterization will be performed using techniques such as SEM and TEM to determine the degree of pore-filling and film uniformity, and XRD to determine crystal structure and crystallinity. Scanning probe microscopy will be used to determine grain boundary and junction properties such as surface photovoltage at the nanometer length scale. XPS studies could be useful to determine the composition and bonding character of the surface species present before and after etching processes and buffer layer deposition.

Optical absorption and photoluminescence will be performed to determine absorption coefficients and band gaps. DLTS, deep-level transient spectroscopy could also be utilized to measure the non-radiative recombination centers (performed at Accent Optical, San Jose, CA), and spectral CL mapping could be used to determine uniformity and threading dislocation density (performed at NREL, Golden, CO). The device characterization will include photocurrent-voltage under simulated AM1.5 solar spectrum, spectral quantum efficiency, and capacitance-voltage measurements.

Publications

(none)

References

1. Hultheen, J. C., Van Duyne, R. P. *J. Vac. Sci. Technol. A* **13**, 1553, (1995).
2. Berger, V., Gauthier-Lafaye, O. & Costard, E. *J. Appl. Phys.* **82**, 60 (1997).
3. Diggle, J. W., Downie, T. C. & Goulding, C. W. *Chem. Rev.* **69**, 365, (1969).
4. <http://www.cneu.psu.edu/amps/default.htm>.
5. Kayes, B.M. and Atwater, H.A., *J. Appl. Phys* **97**, 114302 (2005).
6. <http://www.ise.com>.
7. Mane, R. S. and Lokhande, C. D., *Mat. Chem. and Phys.* **65**, 1, (2000).
8. Engelkin, R. S., S. Ali, L. N. Chang, C. Brinkley, K. Turner, and C. Hester, *Mat. Lett.* **10**, 264-74 (1990).
9. Nair, M. T. S., C. Lopéz-Mata, O. Gomez-Daza, and P. K. Nair, *Semicond. Sci. and Tech.* **18** 755 (2003).
10. Nair, P. K., and M. T. S. Nair, *Semicond. Sci. and Tech.* **7**, 239 (1992).
11. Nakada, T., and M. Mizutani, *J. J. Appl. Phys.* **41**, L165 (2002).
12. Jimbo, K., Kimura, R., Kamimura, T., Yamada, S., Maw, W.S., Araki, H., Oishi, K., Katagiri, H., *Thin Solid Films* (2007).
13. Yanfa, Y., et al., *Applied Physics Letter*, **87**, 121904 (2005).
14. Yanfa, Y., R. Noufi, and M.M. Al-Jassim, *Physical Review Letters*, **96**, 205501 (2006).
15. Nanu, M., Schoonman, J., and Goossens, A., *Nano Lett.* **5**(9), 1716-1719 (2005).
16. Nanu, M., Schoonman, J., and Goossens, A., *Adv. Func. Mat.* **15**(1), 95-100 (2005).
17. Green, M.A., et al., *Prog. Photovolt: Res. Appl.* **14**, 45-51 (2006).

Contacts

Stacey Bent, sbent@stanford.edu
James S. Harris, harris@snowmass.stanford.edu
Michael McGehee, mmcgehee@stanford.edu